
⁶⁴Cu-Labeled Peptide for PET of Breast Carcinomas Expressing the Thomsen-Friedenreich Carbohydrate Antigen

Senthil R. Kumar^{1,2}, Fabio A. Gallazzi³, Thomas P. Quinn¹, and Susan L. Deutscher^{1,2}

¹Department of Biochemistry, University of Missouri–Columbia School of Medicine, Columbia, Missouri; ²Harry S. Truman Veterans Hospital, Columbia, Missouri; and ³Department of Chemistry, University of Missouri, Columbia, Missouri

Thomsen-Friedenreich (TF) antigen is a disaccharide, galactose β 1-3 *N*-acetylgalactosamine (Gal β 1-3GalNAc), expressed on the cell surfaces of most human carcinomas including breast. In this study, we synthesized and evaluated the *in vitro* and *in vivo* properties of a ⁶⁴Cu-radiolabeled TF antigen-specific peptide derived from bacteriophage display for the purpose of breast tumor targeting and PET of human breast tumors in xenografted mice. **Methods:** The TF antigen-specific peptide IVWHRWYAWSPASRI was synthesized with the chelator 1,4,7-triazacyclononane-1,4,7-triacetic acid (NOTA) at the amino terminus, followed by a Gly-Ser-Gly (GSG) spacer. Amino acids Asp and Arg were introduced at both ends to enhance its solubility. Purified NO2A-GSG-DRD-IVWHRWYAWSPASRI-DRD (NO2A-TFpеп) was radiolabeled with ⁶⁴Cu and evaluated for binding to human MDA-MB-435 breast cancer cells, 50% inhibitory concentration (IC₅₀), and serum stability. *In vivo* pharmacokinetic and small-animal PET studies were performed using SCID mice bearing MDA-MB-435 tumor xenografts. **Results:** ⁶⁴Cu-NO2A-TFpеп bound to human MDA-MB-435 breast carcinoma cells, whereas almost no binding was observed to normal human breast 184A1 cells. The peptide exhibited an apparent IC₅₀ value of 70 \pm 8.0 nM. *In vivo* biodistribution studies indicated radiolabeled peptide accumulation in tumors of MDA-MB-435 xenografted SCID mice of approximately 1.10 \pm 0.20 percentage injected dose per gram (%ID/g) and 0.90 \pm 0.12 %ID/g, at 0.5 and 1 h, respectively. Accumulation of radioactivity was low in other organs, with the exception of liver (1.52 \pm 0.12 %ID/g) and kidneys (15.4 \pm 1.73 %ID/g) at 1 h. Live imaging studies with ⁶⁴Cu-NO2A-TFpеп (15 MBq) demonstrated good tumor uptake at 1 h after injection, whereas no tumor uptake was observed with a scrambled radiolabeled peptide ⁶⁴Cu-NO2A-GSG-DRD-RWSWWAVHRI-PYSAI-DRD. **Conclusion:** ⁶⁴Cu-NO2A-TFpеп may function as a noninvasive *in vivo* tumor imaging agent of human breast and other carcinomas expressing the TF carbohydrate antigen. This is the first such TF antigen-targeting peptide used in tumor imaging.

Key Words: TF antigen; imaging; PET; breast carcinoma; radiolabeling

J Nucl Med 2011; 52:1819–1826
DOI: 10.2967/jnumed.111.093716

Thomsen-Friedenreich (TF) antigen is a well-established tumor-associated antigen discovered in the late 1920s (1). The reactive portion of TF antigen is the terminal carbohydrate moiety galactose β 1-3 *N*-acetylgalactosamine (Gal β 1-3GalNAc), which is exposed on proteins and lipids in cancer cells but is masked by a sialic acid on healthy cells (2). TF antigen occurs on approximately 90% of human carcinomas, including those of the breast, colon, lung, bladder, and prostate (1,3–5), and correlates with cancer progression and metastasis (2). Previously, we reported that TF antigen in nipple aspirate fluid from breast carcinoma patients may facilitate breast cancer diagnosis (6,7). Studies from our laboratory also indicated that TF antigen on breast (MDA-MB-435) carcinoma cells is a major ligand of galectin-3 (4). Galectin-3 interactions with TF antigen facilitate cancer cell adhesion and metastasis (4,8). Together these studies suggest that TF antigen is a valuable target for cancer imaging and therapy probe development.

Numerous anti-TF antigen antibodies have been generated (3,9–11). However, most carbohydrate-binding antibodies are large multivalent IgM molecules (12) with physical or chemical characteristics that limit their applications (13). Recent studies reported the isolation of single-chain antibodies (14) and peptides (15) from bacteriophage (phage) display libraries for use in cancer diagnosis and carbohydrate detection, respectively. We identified a TF antigen-binding peptide (HGRFILPWWYAFSPS, P-30) from a phage display library (16). Although P-30 inhibited carcinoma cell aggregation when tested *in vitro* with MDA-MB-435 breast carcinoma cells (17), its use was limited because of low affinity and poor solubility (16). A second-generation peptide, IVWHRWYAWSPASRI (P30-1), was selected from a microlibrary containing the TF antigen-binding motif (W-Y-A-W/F-S-P) (18). This peptide exhibited slightly improved solubility, compared with P-30,

Received May 24, 2011; revision accepted Jul. 29, 2011.
For correspondence contact: Susan L. Deutscher, Department of Biochemistry, 117 Schweitzer Hall, Columbia, MO 65211.
E-mail: deutscher@missouri.edu
Published online Oct. 7, 2011.
COPYRIGHT © 2011 by the Society of Nuclear Medicine, Inc.

with an *in vitro* affinity of 581 ± 98 nM, and inhibited the interaction of TF antigen with galectin-3 (17,19).

It is hypothesized that the second-generation TF antigen-binding peptide P30-1 can be developed into a molecular imaging agent for detection of TF antigen-expressing breast carcinomas. In the present study, TF antigen-binding peptide IVWHRWYAWSPASRI (P30-1) was synthesized with Asp-Arg-Asp (DRD) at both amino and carboxy terminal ends to increase its solubility. The resultant peptide was conjugated with a Gly-Ser-Gly (GSG) spacer (GSG-DRD-IVWHRWYAWSPASRI-DRD, TFpеп) to a chelator, 1,4,7-triazacyclononane-1,4,7-triacetic acid (NOTA). The NOTA-derivatized peptide NO2A-GSG-DRD-IVWHRWYAWSPASRI-DRD (herein referred to as NO2A-TFpеп) was radiolabeled with ^{64}Cu because this radionuclide has favorable properties for use in PET and radiotherapy due to its half-life (12.7 h), decay characteristics (beta positron emission [β^+ ; 19%]; beta electron emission [β^- ; 39%]), and ability for cyclotron production with high specific activity. The radiolabeled ^{64}Cu -NO2A-TFpеп was evaluated for *in vitro* cell binding in human MDA-MB-435 breast carcinoma cells and *in vivo* biodistribution and PET capability in human MDA-MB-435 breast tumor heterotransplanted severe combined immunodeficiency (SCID) mice. MDA-MB-435 cells were used because they express high levels of TF antigen and readily form breast tumors in mice (4,17). To the best of our knowledge, this study is the first to demonstrate the noninvasive imaging of TF antigen on tumors using a small molecule such as ^{64}Cu -NO2A-TFpеп.

MATERIALS AND METHODS

Chemicals and Reagents

^{64}Cu (half-life, 12.7 h; specific activity, 9.398 TBq/mMol [~ 254 Ci/mMol]) was purchased from the Nuclear Reactor Laboratory, University of Wisconsin. Copper purity was 99.91%, with little trace metal impurities ($\sim 0.09\%$). NOTA was procured from Chematech. Reversed-phase high-performance liquid chromatography (RP-HPLC) grade acetonitrile and trifluoroacetic acid were purchased from Fischer Scientific. Cell-growth RPMI 1640 medium and human mammary epithelial cell medium were purchased from Invitrogen-Gibco. All other chemicals were purchased from Fischer Scientific, unless otherwise mentioned.

Peptide Synthesis

The peptide TFpеп or its scrambled version, TFscr, was synthesized using an Advanced ChemTech 396 multiple peptide synthesizer (Advanced ChemTech) with solid-phase Fmoc chemistry. Protected NO2AtBu (di-*tert*-butyl 2,2'-(1,4,7-triazacyclononane-1,4-diyl)diacetate) was purchased from Chematech and was used to prepare NOTA(tBu)₂ (2-(4,7-bis(2-(*tert*-butoxy)-2-oxoethyl)-1,4,7-triazonan-1-yl)acetic acid) with the N terminus of the peptide on the resin. The bromoacetylated peptidyl resin intermediate was prepared by reacting the N terminus of the protected peptide with bromoacetyl bromide in the presence of diisopropylethylamine, followed by SN₂ reaction of the bromine with NO2AtBu in diisopropylethylamine, yielding NO2A (tBu)₂-peptidyl resin. The NO2A-peptide was cleaved from the resin and deprotected by reaction with trifluoroacetic acid and scavengers. The result-

ing NO2A-peptide conjugates were purified using RP-HPLC on a C18 column (218TP54; Vydac), lyophilized, and stored at -20°C before use. Identities of the peptides were confirmed by electrospray ionization mass spectrometry. The peptide conjugates were peak-purified to 98% or greater before *in vitro* cell-binding assays. A biotinylated version, biotin-GSG-DRD-IVWHRWYAWSPASRI-DRD, of the TFpеп (biotin-TFpеп) was also synthesized and purified.

Radiolabeling of Peptides

Radiolabeling of NO2A-TFpеп and NO2A-TFscr with ^{64}Cu was performed as follows. Peptides (40 μg) were radiolabeled with 30 MBq of ^{64}Cu in ammonium acetate (0.4 M), pH 6.8, in a final volume of 100 μL at 75°C for 60 min. To minimize peptide oxidation, the reaction buffer was purged with nitrogen before radiolabeling. Once radiolabeled, the peptides were purified using a Jupiter column (5 μm , C18, 30 nm [300 \AA], 250×4.6 mm; Phenomenex) and RP-HPLC (10%–95% acetonitrile/0.1% trifluoroacetic acid) for 25 min to separate them from their nonradiolabeled counterparts, concentrated using Empore high-efficiency (C₁₈) extraction disk cartridges, and eluted with 500 μL of 8:2 ethanol/sterile saline. The ethanol was evaporated under nitrogen and diluted to 100 μL with sterile saline. Radiochemical yield for ^{64}Cu -NO2A-TFpеп and ^{64}Cu -NO2A-TFscr was 58% and 52%, respectively. Both ^{64}Cu -peptide conjugates were obtained with 98% or greater purity.

Peptide Conjugation with Nonradioactive Copper

Copper-NO2A-TFpеп conjugate was generated by adding 5 mM CuCl_2 in 0.05 N HCl (100 nmol) to a tube containing purified peptide (90 nmol) and dissolved in 300 μL of ammonium acetate buffer (0.4 M). The pH was adjusted to approximately 6.9 by addition of NaOH and then incubated at 78°C for 60 min and allowed to cool to room temperature. Unbound metal was quenched by adding 50 μL of diethylenetriaminepentaacetic acid (10 mM). Copper-NO2A-TFpеп was purified by RP-HPLC and was determined to be at least 98% pure. Electrospray ionization mass spectrometry was performed to confirm the integrity of the peptides. A similar procedure was performed with the scrambled version of the peptide.

Cell-Binding Studies

The normal mammary 184A1 cell line was obtained from American Type Culture Collection, and cells were grown in human mammary epithelial cell medium supplemented with bovine pituitary extract. MDA-MB-435 cells (obtained from J.E. Price, M.D. Anderson) were maintained as monolayer cultures in RPMI 1640 medium supplemented with 10% fetal bovine serum, sodium pyruvate, nonessential amino acids, and L-glutamine. Cell cultures were maintained at 37°C in a 5% CO_2 humidified incubator. MDA-MB-435 and 184A1 cells grown in culture flasks were trypsinized, released, and washed once in cell-binding medium (RPMI 1640 with 25 mM *N*-(2-hydroxyethyl)piperazine-*N'*-(2-ethanesulfonic acid), pH 7.4, 0.2% bovine serum albumin [BSA], and 3 mM 1,10-phenanthroline). Cells (2×10^5 cells per tube) were transferred to microcentrifuge tubes containing 0.3 mL of cell-binding medium and were incubated at 37°C for different times (10, 20, 30, 40, and 60 min) with 1×10^5 counts per min (cpm) of radiolabeled and scrambled peptide. After incubation, medium was removed and the cells were rinsed with ice-cold 0.01 M phosphate-buffered saline (PBS), pH 7.4, and 0.2% BSA, and then centrifuged. This process was repeated 3 times.

Cell-bound radioactivity was quantitated using a Wallac γ -counter (PerkinElmer Inc.). Cell binding was reported as total radioactivity (cpm) bound to cells. Human MDA-MB-435 breast carcinoma cells were originally isolated from a pleural effusion of a woman with metastatic breast adenocarcinoma (20).

A competitive binding assay with ^{64}Cu -NO2A-TFpеп was performed using cultured MDA-MB-435 breast carcinoma cells to determine 50% inhibitory concentration (IC_{50}). MDA-MB-435 cells (2.5×10^6 cells per tube) were incubated for 45 min at 37°C with 3.0×10^4 cpm of peptide and increasing concentrations of nonradioactive copper-NO2A-TFpеп (10^{-12} to 10^{-5} M) ($n = 3$). The cell-associated radioactivity was measured in a Wallac γ -counter, and the binding affinity was determined by the Graft software program (Erithacus Software Limited).

For fluorescent cell-binding studies, MDA-MB-435 and 184A1 cells were grown on LabTek chamber slides (Nunc Nalgene International), fixed with 3% paraformaldehyde for 30 min, and permeabilized with cold methanol for 15 min. After being washed with 0.01 M PBS, the slides were incubated with 2 μM biotin-TFpеп in 0.01 M PBS, pH 7.5, and 1% BSA for 5 h at room temperature. After 3 washes with 0.01 M PBS, neutravidin-AlexaFlour-488 (10 $\mu\text{g}/\text{mL}$) (Molecular Probes) in 0.01 M PBS, pH 7.5, and 0.5% BSA was added for 1 h at room temperature in the dark. The slides were washed and incubated with 4'-6-diamidino-2-phenylindole for 15 min at room temperature for nuclear staining. After additional washes, the samples were mounted under a coverglass and analyzed on a Bio-Rad MRC confocal microscope.

Biodistribution of ^{64}Cu -NO2A-TFpеп in Human MDA-MB-435 Xenografted SCID Mice

Animal studies were conducted in accordance with protocols approved by the Institutional Animal Care and Use Committee in accordance with U.S. Public Health Service guidelines. SCID female mice (4–5 wk) were obtained from Taconic Farms. Each SCID mouse was subcutaneously inoculated in the right shoulder with 1×10^7 MDA-MB-435 cells, and tumors were allowed to grow for 3–4 wk. Mice bearing MDA-MB-435 tumors ($n = 4$ per time point) were injected with approximately 0.185 MBq of ^{64}Cu -NO2A-TFpеп. Animals were sacrificed at 0.5, 1, 2, 4, and 24 h after injection, after which the tissues and organs of interest were collected and weighed, and radioactivity was counted with a γ -counter. Gastrointestinal tract contents were not removed. Uptake of radioactivity in the tumor and normal tissues and organs was expressed as a percentage of the injected radioactive dose per gram (%ID/g). Whole-blood %ID or %ID/g was determined assuming the blood accounted for 6.5% of the body weight of the mouse. For tumor blocking experiments, MDA-MB-435 breast tumor-bearing mice ($n = 4$) were preinjected with 200 μg of copper-NO2A-TFpеп. At 5 min after injection of the nonradiolabeled peptide, 0.185 MBq of ^{64}Cu -NO2A-TFpеп was injected, and the blocking efficiency was evaluated after 2 h. Also, inhibition experiments with albumin fragments were performed to reduce kidney retention essentially as described (21). Approximately 200 μg of approximately 3- to 50-kDa albumin fragments were preinjected via the tail vein into MDA-MB-435 breast tumor-bearing SCID mice ($n = 3$) 5 min before injection of ^{64}Cu -NO2A-TFpеп. After the animals were sacrificed, kidney uptake of the radiolabeled peptide was determined and expressed as %ID/g. The percentage inhibition of the radiolabeled peptide

uptake in the presence of albumin fragments was assessed after comparing it with control animals without preinjection of albumin fragments.

Serum Stability and Metabolism of ^{64}Cu -NO2A-TFpеп

In vitro serum stability was tested by incubating 37.0 MBq of ^{64}Cu -NO2A-TFpеп in 0.3 mL of mouse serum at 37°C for 1, 2, and 24 h. After incubation, the samples were passed through a 0.22- μM filter (Millipore). An aliquot (40 μL) was removed, and the serum proteins were precipitated with 40 μL of acetonitrile. After centrifugation (12,500 rpm for 5 min), cleared supernatant (40 μL , 4.9 MBq) was analyzed by RP-HPLC with a 0%–95% acetonitrile gradient for 25 min to assess the integrity of the radioconjugates. It is possible that there was some retention of the radioactivity in the filters and in the precipitated protein pellet especially during longer incubation times.

In vivo metabolic stability of ^{64}Cu -NO2A-TFpеп was tested by administering 30.0 MBq of the radioactive peptide by tail vein injection into a tumor-bearing SCID mouse. At 1 and 2 h, a urine specimen from the mice was collected and centrifuged to sediment any precipitate, and after being passed through a 0.22- μM filter (Millipore), an aliquot (9.4 MBq) was analyzed by RP-HPLC to determine the radiolabeled peptide peak integrity.

Small-Animal PET/CT Studies

Mice bearing MDA-MB-435 tumors were imaged by small-animal PET/CT. MDA-MB-435 tumor-bearing mice were injected in the tail vein with 15.0 MBq of ^{64}Cu -NO2A-TFpеп or ^{64}Cu -NO2A-TFscr and imaged at 1 h after injection in a small-animal PET scanner (Inveon PET; Siemens) under isoflurane anesthesia. Small-animal PET images were reconstructed using an ordered-subset expectation maximization 2-dimensional algorithm. For the purpose of anatomic-molecular data fusion, small-animal CT was performed and concurrent images were reconstructed with a Fanbeam (Feldkamp) filtered-backprojection algorithm. PET/CT image fusion and visualization was accomplished using Inveon Research Workplace Software (Siemens Inveon Software).

Statistical Analysis

The data are presented as mean \pm SD. For statistical analysis, a Student *t* test was performed using Prism software (GraphPad Software). A *P* value of 0.05 or less was considered significant.

RESULTS

Synthesis and Characterization of Peptides

The peptides NO2A-TFpеп and NO2A-TFscr were synthesized using solid-phase peptide synthesis. In Figure 1, the chemical structures of the peptides are shown. After being radiolabeled with ^{64}Cu , the peptides were purified by RP-HPLC. Observed retention times of ^{64}Cu -NO2A-TFpеп and its scrambled version were 13.5 and 13.8 min, respectively, under identical RP-HPLC conditions. Peptides were obtained at high radiochemical purity, with a reasonable radiochemical yield of 58% and 52%, respectively (Table 1). The observed and calculated molecular weight of native copper-NO2A-TFpеп was 3,245.0 and 3,245.8 Da, respectively. Similarly, for native copper-NO2A-TFscr peptide the mass was 3,245.0 Da (calculated) and 3,246.0 Da (observed). The specific activity of ^{64}Cu -NO2A-TFpеп was approximately 17.4 MBq/nmol (0.47 Ci/ μmol).

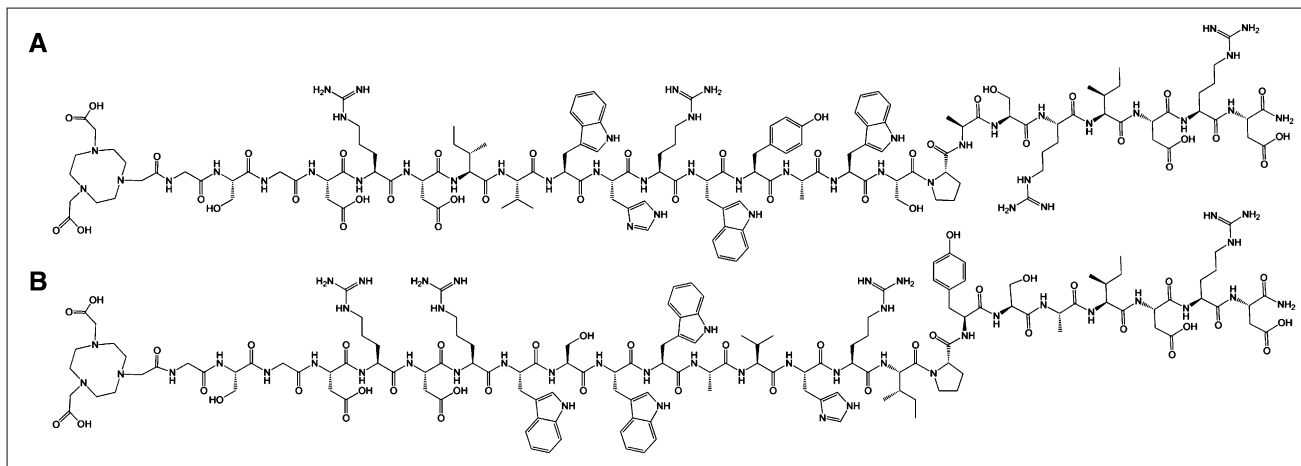


FIGURE 1. Chemical structures of NO2A-TFpеп (A) and NO2A-TFscr (B).

Cell Binding and Serum Stability

Fluorescent cell-binding studies were performed with biotin-GSG-TFpеп using confocal microscopy. Although the peptide bound to TF antigen-positive MDA-MB-435 cells, little binding was observed with normal mammary epithelial 184A1 cells, as shown in Figure 2A. The ability of ^{64}Cu -radiolabeled peptides to bind MDA-MB-435 breast carcinoma cells or 184A1 normal mammary epithelial cells was also tested. The results shown in Figure 2B indicate that the binding of ^{64}Cu -NO2A-TFpеп to MDA-MB-435 cells occurred in a time-dependent manner. Peptide binding to MDA-MB-435 cells was observed to be high at 20 min, beyond which time it reached a plateau. Cell binding of the peptide was not observed with 184A1 cells. The scrambled peptide exhibited low binding to both cell lines.

In vitro competitive binding studies with ^{64}Cu -NO2A-TFpеп in the presence of its respective nonradioactive counterpart (copper-NO2A-TFpеп) were performed using cultured human MDA-MB-435 breast carcinoma cells. The radiolabeled peptide demonstrated nanomolar affinity to MDA-MB-435 cells with an apparent IC_{50} value of 70 ± 8.0 nM (Table 1). In a separate study, ^{64}Cu -NO2A-TFpеп was incubated in mouse serum for 1, 2, and 24 h in vitro at 37°C . RP-HPLC analysis shown in Figure 3 indicates that the radiolabeled peptide was stable in serum up to 24 h and demonstrated no observable decomposition. We also analyzed the metabolic stability of ^{64}Cu -NO2A-TFpеп in urine at 1 and 2 h, respectively. At both time points, analysis of

urine by RP-HPLC did not reveal any additional metabolites other than the parent peptide (data not shown).

Pharmacokinetics of ^{64}Cu -NO2A-TFpеп in MDA-MB-435 Xenografted SCID Mice

In vivo pharmacokinetic studies were conducted to assess the tumor and normal tissue uptake of the radiolabeled peptide. Results obtained with ^{64}Cu -NO2A-TFpеп in mice bearing MDA-MB-435 breast tumors are summarized in Tables 2 and 3. As shown, most of the radiolabeled peptide cleared through the renal system, with 90.1 ± 0.64 %ID and 94.2 ± 1.15 %ID in the urine at 2 and 24 h after injection, respectively. Although overall clearance of the radiolabeled peptide proceeded primarily through the renal-urinary system, approximately 1.65 ± 0.08 %ID and 1.57 ± 0.3 %ID was excreted through the hepatobiliary system at 2 h and 24 h, respectively. Disappearance of the peptide in blood was rapid from 0.5 h (1.52 ± 0.18 %ID/g) up to 2 h (0.15 ± 0.02 %ID/g), beyond which no significant changes until 24 h (0.1 ± 0.02 %ID/g) were noticed, suggesting a short residence time for the radiolabeled peptide in the blood.

Tumor uptake of ^{64}Cu -NO2A-TFpеп was comparable at 0.5 h (1.10 ± 0.20 %ID/g), 1 h (0.90 ± 0.12 %ID/g), and 2 h (0.84 ± 0.06 %ID/g). However, at 4 h and beyond, there was a decline in the tumor retention of the radiolabeled peptide. Tumor blocking studies were performed with 200 μg of copper-NO2A-TFpеп 5 min before the injection of its radiolabeled counterpart in MDA-MB-435 xenografted

TABLE 1
Characterization of ^{64}Cu -Labeled Peptides

Peptide	RP-HPLC (t_r -min)	Labeling yield (%)	Radiochemical purity	Receptor affinity (IC_{50}) (nM)
^{64}Cu -NO2A-TFpеп	13.5	58	≥ 98	70 ± 8.0
^{64}Cu -NO2A-TFscr	13.8	52	≥ 97	—

IC_{50} was determined using copper-NO2A-TFpеп as competitor.

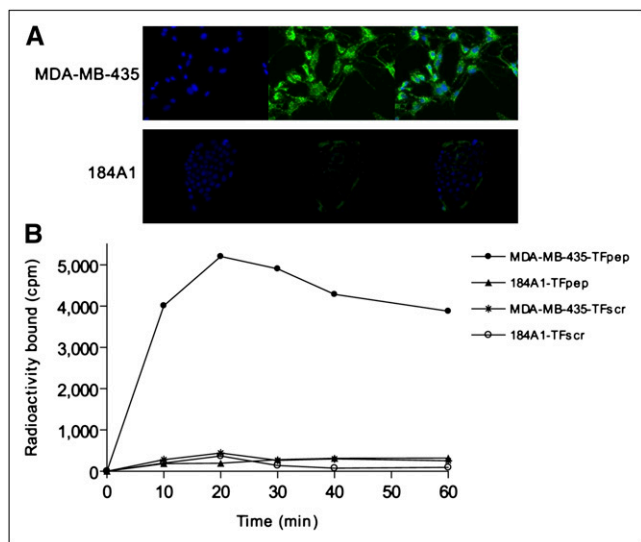


FIGURE 2. (A) Fluorescence cell-binding analysis. TF antigen-expressing human MDA-MB-435 breast carcinoma cells and 184A1 normal mammary epithelial cells were grown in chamber slides, and after fixing, slides were incubated for 5 h with 2 μ M biotin-TFpép at room temperature. Cell-bound peptide was detected using neutravidin-AlexaFlour 488 (10 μ g/mL). 4'-6-diamidino-2-phenylindole was used for nuclear staining. Slides were analyzed using Bio-Rad MRC confocal microscope: nuclear staining with 4'-6-diamidino-2-phenylindole (left), fluorescent staining with neutravidin-AlexaFlour 488 (middle), and merged image (right). (B) MDA-MB-435 or 184A1 cells (2×10^5 cells per tube) were suspended in cell-binding medium and incubated at 37°C for different times (10–60 min) with 1×10^5 cpm of $^{64}\text{Cu-NO}_2\text{A-TFpép}$ or $^{64}\text{Cu-NO}_2\text{A-TFs}_{cr}$, respectively. After incubation, medium was removed and cells were washed and centrifuged. Cell-bound radioactivity was quantified using Wallac γ -counter. Data are presented as mean \pm SD, with each point being performed in triplicate.

mice ($n = 3$). Another set of mice ($n = 3$) was injected with $^{64}\text{Cu-NO}_2\text{A-TFpép}$ only, serving as a positive control. The results demonstrated that specific tumor uptake of radiolabeled peptide was blocked by 55% (Tables 2 and 3). At 2 h, the

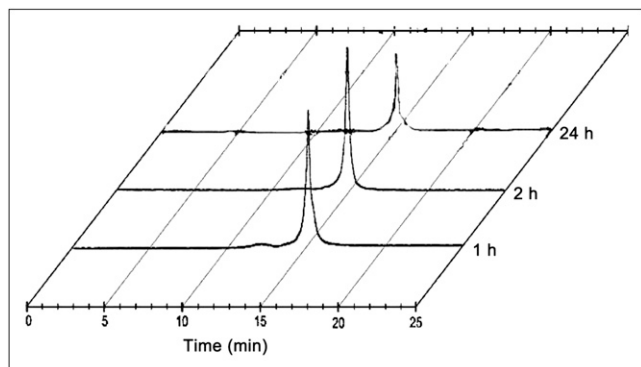


FIGURE 3. Serum stability studies of $^{64}\text{Cu-NO}_2\text{A-TFpép}$. In vitro serum stability of $^{64}\text{Cu-NO}_2\text{A-TFpép}$ was tested by incubating 37.0 MBq of peptide in 0.3 mL of mouse serum at 37°C for 1, 2, and 24 h, respectively. After incubation, samples were filtered (0.22- μ M filter). After precipitation of serum proteins, cleared supernatant (4.9 MBq) was analyzed by RP-HPLC with 0%–95% gradient acetonitrile.

tumor-to-blood (5.60) and tumor-to-muscle ratios (28.0) were higher than the tumor-to-liver ratio (0.64), suggesting that the clearance of radioconjugate from nontarget tissues such as muscle and blood was faster than from liver (Table 3). Excess cold peptide injection did not affect kidney retention.

Kidney retention of the radiolabeled conjugate was found to be high at 0.5 h, followed by a gradual decrease up to 4 h and a significant reduction at 24 h. Compared with initial peptide uptake at 0.5 h, the reduction in kidney uptake was 1.6-fold (2 h), 2.5-fold (4 h), and 11.4-fold (24 h), respectively. To reduce the kidney retention of the radiolabeled peptides, albumin fragments were used as blocking agents (21). Figure 4 shows the renal uptake of the radiolabeled peptides with and without albumin fragments. The retention of the radiolabeled peptide in the kidney was blocked in the presence of albumin fragments by 49% ($n = 3$, $P = 0.042$).

Small-Animal PET/CT Studies

Small-animal PET/CT experiments were performed in SCID mice bearing MDA-MB-435 tumors. Mice were injected intravenously with 15.0 MBq of $^{64}\text{Cu-NO}_2\text{A-TFpép}$ or $^{64}\text{Cu-NO}_2\text{A-TFs}_{cr}$, and live images were acquired at 1 h after injection (Fig. 5). In the animal injected with $^{64}\text{Cu-NO}_2\text{A-TFpép}$ (Fig. 5A), tumors could be easily visualized in the fused small-animal PET/CT whole-body image. Uptake of peptide was also observed in the abdomen, probably because of retention of radioactivity in the gastrointestinal tract and liver, as well as in the kidneys. With $^{64}\text{Cu-NO}_2\text{A-TFs}_{cr}$, however, no tumor uptake was observed (Fig. 5B), whereas uptake in organs was similar to that of $^{64}\text{Cu-NO}_2\text{A-TFpép}$, with abdominal uptake being slightly higher. Prominent nontarget uptake of the radiola-

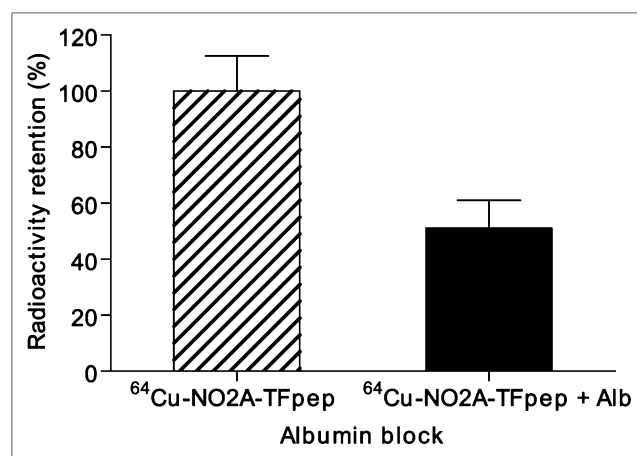


FIGURE 4. Renal radioactivity retention of $^{64}\text{Cu-NO}_2\text{A-TFpép}$ with albumin fragments. Albumin fragments obtained by tryptic digestion (200 μ g) were preinjected in mice 5 min before injection of radiolabeled peptide (0.185 MBq). In vivo kidney uptake of radiolabeled peptide in mice administered with or without albumin fragments was measured in γ -counter. Renal retention of $^{64}\text{Cu-NO}_2\text{A-TFpép}$ was 49% ($n = 3$, $P = 0.042$) in presence of albumin fragments. Alb = albumin.

TABLE 2
Biodistribution of ⁶⁴Cu-NO2A-TFpеп Using MDA-MB-435 Tumor-Bearing SCID Mice

Tissue	Time					
	0.5 h	1 h	2 h	2-h block	4 h	24 h
Tumor	1.10 ± 0.20	0.90 ± 0.12	0.84 ± 0.06	0.38 ± 0.09*	0.28 ± 0.04	0.19 ± 0.02
Blood	1.52 ± 0.18	0.33 ± 0.10	0.15 ± 0.02	0.11 ± 0.02	0.12 ± 0.03	0.10 ± 0.02
Brain	0.05 ± 0.01	0.02 ± 0.00	0.01 ± 0.00	0.02 ± 0.00	0.02 ± 0.00	0.04 ± 0.00
Heart	0.40 ± 0.05	0.16 ± 0.06	0.04 ± 0.01	0.13 ± 0.02	0.04 ± 0.02	0.07 ± 0.02
Lung	2.17 ± 0.23	0.58 ± 0.04	0.43 ± 0.04	0.37 ± 0.04	0.30 ± 0.08	0.27 ± 0.08
Liver	1.87 ± 0.32	1.52 ± 0.12	1.31 ± 0.20	1.30 ± 0.20	1.28 ± 0.08	1.26 ± 0.20
Spleen	0.62 ± 0.11	0.27 ± 0.04	0.32 ± 0.09	0.29 ± 0.02	0.27 ± 0.03	0.30 ± 0.10
Stomach	0.47 ± 0.21	0.23 ± 0.05	0.30 ± 0.05	0.29 ± 0.05	0.29 ± 0.06	0.19 ± 0.07
Kidneys	23.18 ± 4.41	15.38 ± 1.73	14.15 ± 2.30	13.8 ± 1.08	9.37 ± 0.87	2.04 ± 0.64
Muscle	0.30 ± 0.12	0.08 ± 0.01	0.03 ± 0.01	0.03 ± 0.00	0.05 ± 0.03	0.04 ± 0.02
Pancreas	0.51 ± 0.13	0.17 ± 0.07	0.16 ± 0.07	0.12 ± 0.03	0.14 ± 0.08	0.10 ± 0.05
Bone	0.22 ± 0.08	0.17 ± 0.03	0.09 ± 0.04	0.09 ± 0.05	0.02 ± 0.01	0.03 ± 0.00
Intestines	1.28 ± 0.37	0.95 ± 0.07	1.40 ± 0.34	1.30 ± 0.60	1.31 ± 0.35	1.29 ± 0.47
Urine	73.7 ± 8.92	86.9 ± 2.70	90.1 ± 0.64	90.9 ± 1.06	90.4 ± 0.47	94.2 ± 1.15

**P* = 0.002, significant, compared with ⁶⁴Cu-NO2A-TFpеп uptake in absence and presence of its nonradioactive copper-labeled counterpart at 2 h after injection.

Data presented are %ID/g ± SD, except for intestines and urine, which are %ID ± SD (*n* = 4).

beled peptides in the kidneys suggests that these tracers are mainly excreted through this organ.

DISCUSSION

In the present study, we examined if a phage display-derived TF antigen-binding peptide could target and PET image TF antigen-expressing breast tumors in vivo. Previously we reported that human breast (MDA-MB-435) car-

cinoma cell lines express TF antigen on their surfaces and demonstrated the participation of TF antigen in MDA-MB-435 carcinoma cell adhesion to the endothelium (4). For PET agent development, we conjugated the TFpеп to the polydentate macrocyclic ligand NOTA. The NOTA-derivatized conjugate NO2A-TFpеп, when radiolabeled with ⁶⁴Cu, exhibited specific binding to MDA-MB-435 human breast carcinoma cells. The tumor-targeting and imaging abilities of this peptide in vivo were demonstrated by pharmacokinetic studies and small-animal PET experiments. The only other PET study of TF antigen was using ¹²⁴I-iodine-labeled JAA-F11, an IgG3 monoclonal antibody (22). Although radiolabeled IgG3-JAA-F11 binding to the tumor was visualized in PET, its blood half-life was long (2.4 d), and imaging was successful only after 48 h, apparently because of high levels of antibody in the blood (22).

We chose to use the chelator NOTA because recent studies have shown its kinetic inertness when radiolabeled with divalent metals in vivo (23), compared with tetramine macrocyclic chelators such as DOTA or 1,4,8,11-tetraazacyclotetradecane-1,4,8,11-tetraacetic acid (TETA) (23). The NOTA derivative, NO2A, was shown to bind well to ⁶⁴Cu while conjugated to a functional biomolecule (23).

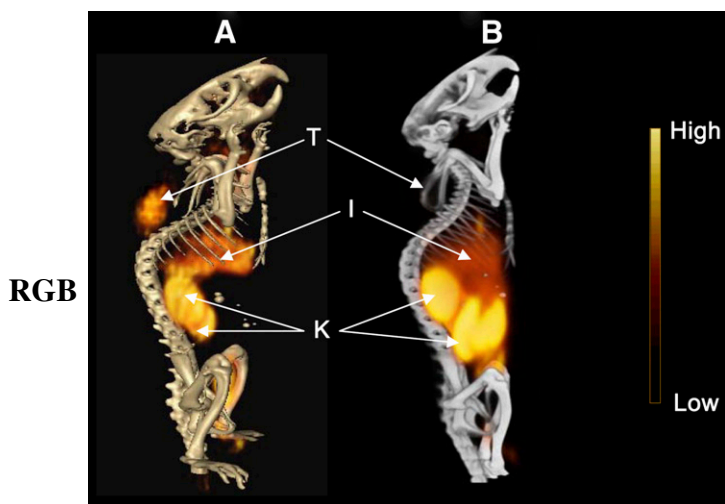


FIGURE 5. Small-animal imaging studies with MDA-MB-435 tumor-bearing SCID mice. ⁶⁴Cu-NO2A-TFpеп or ⁶⁴Cu-NO2A-TFscr (15.0 MBq) was injected into tail vein of SCID mice bearing MDA-MB-435 tumor xenografts. Live imaging was acquired at 1 h after injection, under isoflurane anesthesia in Siemens PET scanner. To validate regions of increased radiolabeled peptide uptake, PET images were fused with conventional micro-CT images. Figures depict left lateral fused PET/CT images with ⁶⁴Cu-NO2A-TFpеп (A) and ⁶⁴Cu-NO2A-TFscr (B). I = intestine; K = kidney; T = tumor.

TABLE 3
Uptake Ratio of Tumor to Normal Tissue

Uptake of...	Time					
	0.5 h	1 h	2 h	2-h block	4 h	24 h
Tumor to blood	0.72	2.72	5.60	—	2.30	1.90
Tumor to muscle	3.66	11.25	28.00		5.60	4.75
Tumor to liver	0.59	0.80	0.64		0.20	0.15

The ^{64}Cu -NO₂A-TFpep bound to TF antigen-expressing human MDA-MB-435 breast carcinoma cells in a sequence-specific manner whereas it did not bind normal mammary epithelial cells 184A1. ^{64}Cu -NO₂A-TFscr did not bind to either MDA-MB-435 or 184A1 cells, suggesting that altering the peptide sequence hampered peptide binding to TF antigen-expressing cells. Competition studies in vitro with a nonradiolabeled counterpart demonstrated specificity of the radiolabeled peptide for MDA-MB-435 cultured breast carcinoma cells (IC_{50} , 70 ± 8.0 nM).

In vivo pharmacokinetic studies demonstrated tumor uptake of ^{64}Cu -NO₂A-TFpep. The in vivo tumor blocking studies revealed a partial block in the uptake of ^{64}Cu -NO₂A-TFpep in the presence of copper-NO₂A-TFpep. Such partial tumor block might be attributed to the rapid disappearance of the competing peptide in circulation, thus reducing its residence time, or rapid uptake in nontarget tissues including the kidney. With the exception of the liver and kidneys, the disappearance of radiotracer from blood and other nontarget tissues indicated clearance of the peptide complex from these tissues. However, from 1 to 24 h, the tumor-to-liver ratio was relatively lower than tumor-to-blood or tumor-to-muscle ratios, suggesting some ^{64}Cu retention in the liver. Previous studies have speculated that the NOTA chelating ability of ^{68}Ga is higher than that of ^{64}Cu because of liver retention with NOTA-RGD-bombesin peptides labeled with these radiometals (23). On the basis of the tumor-to-liver ratio values obtained in our studies, we speculate that some ^{64}Cu dissociation could have occurred in the liver. An earlier study reported accumulation of ^{64}Cu -NOTA-8-AOC-bombesin(7-14)NH₂ in liver that was lower than ^{64}Cu -DOTA-AOC-bombesin(7-14)NH₂ retention in the liver (24). Also, Bass et al. observed dissociation of the ^{64}Cu radionuclide from DOTA or TETA chelators in vivo and retention of radioactivity in the liver (25).

Kidney retention of the radiolabeled peptide was high until 2 h. Radiometal-chelated amino acids can be trapped in the renal tubular cell lysosomes, which may result in significant radiation dose to the kidneys (26). Vegt et al. demonstrated that albumin fragments reduced renal uptake of ^{111}In -labeled octreotide, exendin, and minigastrin by 30%, 52%, and 93%, respectively (21,27). We observed a partial block (50%) in retention of ^{64}Cu -NO₂A-TFpep in the kidneys using similar albumin blocking studies, suggesting that there are multiple mechanisms in tubular absorption of radiolabeled peptides (28). Thus, it is likely that a multitargeted approach may be necessary to reduce kidney retention of ^{64}Cu -NO₂A-TFpep.

The small-animal PET/CT images obtained at 1 h after injection in MDA-MB-435 human breast tumor-bearing live mice agreed well with the biodistribution profile. Tumor uptake of ^{64}Cu -NO₂A-TFpep could be easily visualized in PET, confirming the uptake in the biodistribution studies. Parallel studies with the scrambled peptide ^{64}Cu -NO₂A-TFscr revealed no uptake in the tumor tissue. Thus,

alteration in the peptide sequence abolished tumor binding and demonstrated specificity of ^{64}Cu -NO₂A-TFpep. Tumor uptake with ^{64}Cu -NO₂A-TFpep was clearly visible along with abdominal uptake at 1 h after injection. Radioactivity in the intestines could be due to the lipophilicity of the radiolabeled peptide and hepatobiliary clearance of ^{64}Cu -NO₂A-TFpep. Alternatively, ^{64}Cu that transchelated from NOTA to serum proteins could have cleared slowly through the liver and gastrointestinal tract. The kidney retention of ^{64}Cu -NO₂A-TFpep was also clearly visible on PET images. Improvement in the tumor uptake and pharmacokinetics of ^{64}Cu -labeled cyclic RGD peptides using Gly-Gly-Gly (GGG) and polyethyleneglycol 4 (PEG4) linkers has been reported (29). Other studies indicated that prostate tumor uptake of ^{64}Cu -labeled DOTA-bombesin peptide with a GGG-linker was higher than that with a GSG-linker, although kidney uptake was higher (30). Future work will focus on evaluating and optimizing the pharmacokinetic profile of ^{64}Cu -NO₂A-TFpep using more than 1 linker group based on hydrocarbons, PEG, or amino acids.

CONCLUSION

The TF antigen-specific peptide ^{64}Cu -NO₂A-TFpep was evaluated for its pharmacokinetics and PET properties in MDA-MB-435 human tumor-bearing mice. Biodistribution studies and PET demonstrated good tumor uptake with this radioconjugate, although improvement is needed to decrease in vivo kidney retention. Overall, ^{64}Cu -NO₂A-TFpep could function as an effective imaging probe for TF antigen-expressing breast and other carcinomas.

DISCLOSURE STATEMENT

The costs of publication of this article were defrayed in part by the payment of page charges. Therefore, and solely to indicate this fact, this article is hereby marked "advertisement" in accordance with 18 USC section 1734.

ACKNOWLEDGMENTS

We thank Lisa Watkinson and Terry Carmack for help with animal experiments, Marie Dickerson and Xiuli Zhang for technical assistance, and the VA Biomolecular Imaging Center for assisting in the imaging studies. We acknowledge financial support from the National Institutes of Health (1R-21CA137239-01A1), DOE (DE SC0002121), and a Merit Review Award from the Veterans Administration. No other potential conflict of interest relevant to this article was reported.

REFERENCES

1. Springer GF. T and Tn, general carcinoma autoantigens. *Science*. 1984;224:1198-1206.
2. Baldus SE, Zirbes TK, Hanisch FG, et al. Thomsen-Friedenreich antigen presents as a prognostic factor in colorectal carcinoma: a clinicopathologic study of 264 patients. *Cancer*. 2000;88:1536-1543.

3. Rittenhouse-Diakun K, Xia Z, Pickhardt D, Morey S, Baek MG, Roy R. Development and characterization of monoclonal antibody to T-antigen: (gal beta1-3GalNAc-alpha-O). *Hybridoma*. 1998;17:165-173.
4. Glinsky VV, Glinsky GV, Rittenhouse-Olson K, et al. The role of Thomsen-Friedenreich antigen in adhesion of human breast and prostate cancer cells to the endothelium. *Cancer Res*. 2001;61:4851-4857.
5. Janssen T, Petain M, Van Velthoven R, et al. Differential histochemical peanut agglutinin stain in benign and malignant human prostate tumors: relationship with prostatic specific antigen immunostain and nuclear DNA content. *Hum Pathol*. 1996;27:1341-1347.
6. Kumar SR, Sauter ER, Quinn TP, Deutscher SL. Thomsen-Friedenreich and Tn antigens in nipple fluid: carbohydrate biomarkers for breast cancer detection. *Clin Cancer Res*. 2005;11:6868-6871.
7. Deutscher SL, Dickerson M, Gui G, et al. Carbohydrate antigens in nipple aspirate fluid predict the presence of atypia and cancer in women requiring diagnostic breast biopsy. *BMC Cancer*. 2010;10:519-525.
8. Glinsky VV, Glinsky GV, Glinskii OV, et al. Intravascular metastatic cancer cell homotypic aggregation at the sites of primary attachment to the endothelium. *Cancer Res*. 2003;63:3805-3811.
9. Karsten U, Butschak G, Cao Y, Goletz S, Hanisch FG. A new monoclonal antibody (A78-G/A7) to the Thomsen-Friedenreich pan-tumor antigen. *Hybridoma*. 1995;14:37-44.
10. Butschak G, Karsten U. Isolation and characterization of Thomsen-Friedenreich-specific antibodies from human serum. *Tumour Biol*. 2002;23:113-122.
11. Dahlenborg K, Hultman L, Carlsson R, Jansson B. Human monoclonal antibodies specific for the tumour associated Thomsen-Friedenreich antigen. *Int J Cancer*. 1997;70:63-71.
12. Lundquist JJ, Debenham SD, Toone EJ. Multivalency effects in protein-carbohydrate interaction: the binding of the Shiga-like toxin 1 binding subunit to multivalent C-linked glycopeptides. *J Org Chem*. 2000;65:8245-8250.
13. Jain RK. Delivery of novel therapeutic agents in tumors: physiological barriers and strategies. *J Natl Cancer Inst*. 1989;81:570-576.
14. Matsumoto-Takasaki A, Horie J, Sakai K, et al. Isolation and characterization of anti-T-antigen single chain antibodies from a phage library. *Biosci Trends*. 2009;3:87-95.
15. Heimburg-Molinaro J, Almogren A, Morey S, et al. Development, characterization, and immunotherapeutic use of peptide mimics of the Thomsen-Friedenreich carbohydrate antigen. *Neoplasia*. 2009;11:780-792.
16. Peletskaya EN, Glinsky VV, Glinsky GV, Deutscher SL, Quinn TP. Characterization of peptides that bind the tumor-associated Thomsen-Friedenreich antigen selected from bacteriophage display libraries. *J Mol Biol*. 1997;270:374-384.
17. Glinsky VV, Huflejt ME, Glinsky GV, Deutscher SL, Quinn TP. Effects of Thomsen-Friedenreich antigen-specific peptide P-30 on beta-galactoside-mediated homotypic aggregation and adhesion to the endothelium of MDA-MB-435 human breast carcinoma cells. *Cancer Res*. 2000;60:2584-2588.
18. Landon LA, Peletskaya EN, Glinsky VV, Karasseva N, Quinn TP, Deutscher SL. Combinatorial evolution of high-affinity peptides that bind to the Thomsen-Friedenreich carcinoma antigen. *J Protein Chem*. 2003;22:193-204.
19. Zou J, Glinsky VV, Landon LA, Matthews L, Deutscher SL. Peptides specific to the galectin-3 carbohydrate recognition domain inhibit metastasis-associated cancer cell adhesion. *Carcinogenesis*. 2005;26:309-318.
20. Price JE, Polyzos A, Zhang RD, Daniels LM. Tumorigenicity and metastasis of human breast carcinoma cell lines in nude mice. *Cancer Res*. 1990;50:717-721.
21. Vegt E, van Eerd JE, Eek A, et al. Reducing renal uptake of radiolabeled peptides using albumin fragments. *J Nucl Med*. 2008;49:1506-1511.
22. Chaturvedi R, Heimburg J, Yan J, et al. Tumor immunolocalization using 124 I-iodine-labeled JAA- F11 antibody to Thomsen-Friedenreich alpha-linked antigen. *Appl Radiat Isot*. 2008;66:278-287.
23. Prasanphanich AF, Nanda PK, Rold TL, et al. [⁶⁴Cu-NOTA-8-Aoc-BBN(7-14)NH₂] targeting vector for positron-emission tomography imaging of gastrin-releasing peptide receptor-expressing tissues. *Proc Natl Acad Sci USA*. 2007;104:12462-12467.
24. Liu Z, Yan Y, Liu S, Wang F, Chen X. ¹⁸F, ⁶⁴Cu, and ⁶⁸Ga labeled RGD-bombesin heterodimeric peptides for PET imaging of breast cancer. *Bioconjug Chem*. 2009;20:1016-1025.
25. Bass LA, Wang M, Welch MJ, Anderson CJ. In vivo transchelation of copper-64 from TETA- octreotide to superoxide dismutase in rat liver. *Bioconjug Chem*. 2000;11:527-532.
26. Behr TM, Goldenberg DM, Becker W. Reducing the renal uptake of radiolabeled antibody fragments and peptides for diagnosis and therapy: present status, future prospects and limitations. *Eur J Nucl Med*. 1998;25:201-212.
27. Christensen EI, Birn H, Verroust P, Moestrup SK. Megalin-mediated endocytosis in renal proximal tubule. *Ren Fail*. 1998;20:191-199.
28. Gotthardt M, van Eerd-Vismale J, Oyen WJ, et al. Indication for different mechanisms of kidney uptake of radiolabeled peptides. *J Nucl Med*. 2007;48:596-601.
29. Shi J, Kim YS, Zhai S, Liu Z, Chen X, Liu S. Improving tumor uptake and pharmacokinetics of ⁶⁴Cu-labeled cyclic RGD peptide dimers with Gly(3) and PEG(4) linkers. *Bioconjug Chem*. 2009;20:750-759.
30. Parry JJ, Kelly TS, Andrews R, Rogers BE. In vitro and in vivo evaluation of ⁶⁴Cu-labeled DOTA-linker-bombesin(7-14) analogues containing different amino acid linker moieties. *Bioconjug Chem*. 2007;18:1110-1117.